

First Principles Study of a New Large-Gap Nonoporous Silicon Crystal: Hex-Si₄₀

E. Galvani,¹ G. Onida,^{1,2} S. Serra,¹ and G. Benedek¹

¹*Istituto Nazionale per la Fisica della Materia, Dipartimento di Fisica dell'Università di Milano, Via Celoria 16, 20133 Milano, Italy*

²*Istituto Nazionale per la Fisica della Materia, Dipartimento di Fisica dell'Università di Roma Tor Vergata, Via della Ricerca Scientifica, 00133 Roma, Italy*

(Received 17 April 1996)

We present an *ab initio* calculation of the structural and electronic properties of Si in a novel hexagonal, *fourfold* coordinated structure with 40 atoms per unit cell, obtained from the coalescence of small fullerenic cages. Hex-Si₄₀ has a tubular structure, inducing confined electronic states near the gap, which is widened by ~ 0.4 eV with respect to normal silicon. This system is predicted to be a very interesting, possibly photoluminescent material for optoelectronics. [S0031-9007(96)01473-1]

PACS numbers: 61.46.+w, 61.66.Bi, 71.20.Mq

The development of silicon-based optoelectronic devices meets a severe limitation in the fact that, in bulk silicon, the efficiency of interband radiative recombination is low. This is due to the relatively small and indirect energy gap resulting from the band structure of pure silicon. Moreover, the near-gap luminescence peak, located at ~ 1.09 eV, falls below the visible region. A very promising way to overcome this problem has been opened in the 1990's by the discovery of the photoluminescent properties of porous silicon (π -Si) [1]. The precise origin of the efficient, visible light photoluminescence (PL) of π -Si (obtained by etching of Si wafers in HF based electrolytes) has been a matter of debate, and yet not completely clarified [2]. Different possible sources of PL have been considered, both intrinsic and extrinsic, including phonon-assisted mechanisms [3]. The intrinsic mechanism based on quantum confinement effects, originated by the nanoscale filamentary structure of π -Si, is generally accepted as being a source of luminescence, particularly when the confinement occurs on a small length scale ($< 15\text{--}20$ Å). In fact, quantum confinement can induce both a widening of the gap and strong modifications of the energy bands, possibly leading to a direct gap. π -Si has however a quite indeterminate structure, strongly dependent on the fabrication conditions. On the theoretical side, calculations tried to investigate π -Si properties studying either Si nanocrystal [3–5], clusters [6], or nanowires [7].

We have realized and studied these quantum confinement effects in a hypothetical *monolithic* silicon form, where good structural and mechanical properties combine with a good functional reproducibility. We theoretically designed, by means of topological arguments and a density-functional total energy minimization based on the Car-Parrinello method [8,9], a novel crystalline form of silicon having hexagonal symmetry, 40 atoms per unit cell, perfect fourfold coordination, and a regular array of parallel tubes which are able to localize electronic states at the edges of the gap. The electronic structure of this material shows two of the important characteristics which

can lead to visible photoluminescence as in π -Si: (i) a gap widening of more than 0.4 eV and (ii) existence of spatially confined electronic states. This study represents, we believe, a new concept in the design of optical materials, based on structural architecture rather than chemical manipulation.

Guidelines of this work have been the previous theoretical studies on cubic silicon clathrates [10,11], the very recent synthesis of cubic Na₂Ba₆Si₄₆ [12], and our investigations on the topological design of new hollow covalent materials of desired geometry and complexity [13]. The latter studies led us to the discovery of infinite series of fourfold coordinated crystals, which we called “hollow diamonds,” characterized by periodic arrays of cavities whose spacing increases along the series to infinity. Here we are interested in the series of hexagonal hollow silicons hex-Si_{*m*}, with $m = 40[n(n+1)(2n+1)]/6$ and n any natural number [13]. The first ($n = 1$) element of the series, hex-Si₄₀, is a clathrate obtained from the coalescence of two Si₂₆, two Si₂₄, and three Si₂₀ fullerenelike clusters, having the shape of the 15-hedron (3 hexagons and 12 pentagons), 14-hedron (2 hexagons and 12 pentagons) and, dodecahedron, respectively. The unit cell contains $(2 \times 26 + 2 \times 24 + 3 \times 20)/4 = 40$ atoms, and the space group is $P6/mmm$. A perspective view along the c axis of the resulting structure is shown in Fig. 1. The backbone of this lattice is a hexagonal array of parallel tubes, each tube being an infinite pile of Si₂₄ pairs. The tubes are held together by rings of Si₂₆ and Si₂₀ cages arranged on alternate planes normal to the tubes. The Si₂₆ rings form, in each plane, a honeycomb lattice where the Si₂₆ cages are located at the vertices and connected through their hexagonal faces. The Si₂₀ rings also form a honeycomb lattice with the Si₂₀ cages located at the edge midpoints.

We have computed the hex-Si₄₀ equilibrium geometry and electronic structure within the density functional theory (DFT) in the local density approximation (LDA), using a global (ionic + electronic) minimization approach

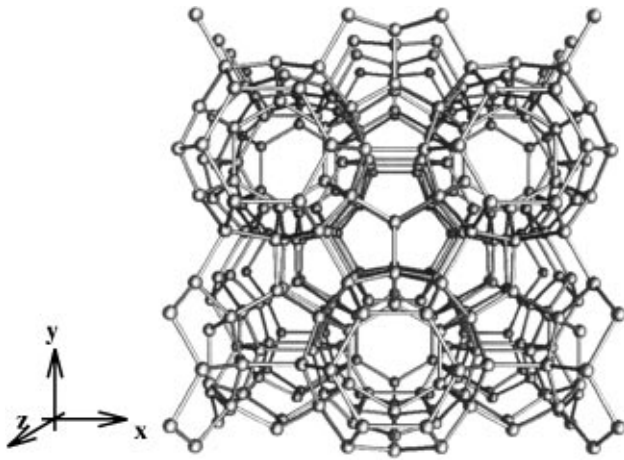


FIG. 1. The structure of hex-Si₄₀, with its characteristic "channels" along the *c* axis.

[14]. A norm-conserving pseudopotential of the Bachelet, Hamann, Schlüter type [15] in the separable Kleinman-Bylander form has been used. The atomic geometry has been optimized with a full relaxation of the internal structure, at several fixed values of the two lattice parameters (*a* and *c/a*). We used an energy cutoff of 11 Ry for the plane wave expansion of the electronic wave functions. Because of the very small volume of the Brillouin zone (BZ), its sampling has been limited to three Chadi-Cohen special points [16]. Convergence in the structural properties has been checked by using the Γ point only, and by increasing the cutoff up to 20 Ry. We have taken, for the sake of comparison, a calculation for normal Si (diamondlike) in a 54 atoms hexagonal supercell, with the same energy cutoff and the same set of *k* points. We obtain for hex-Si₄₀ a cohesive energy of only ~ 0.1 eV/atom below that of normal Si. Because of limited BZ sampling and the use of the LDA, the relative error on such a small energy difference may be large; however, its order of magnitude speaks in favor of the stability of hex-Si₄₀.

At the optimized geometry, hex-Si₄₀ has the structure shown in Fig. 1. Its specific volume is 17.7% larger than in normal silicon, with lattice parameters *a* and *c/a* equal to 10.18 and 1.02 Å, respectively. Eight different bond lengths occur in this lattice, ranging from 2.308 to 2.486 Å, i.e., from 1.8% shorter to 5.8% longer than in diamondlike Si. While basal hexagons are regular by symmetry, vertical hexagons belonging to Si₂₆ are distorted with bond angles of $\sim 126^\circ$ and $\sim 108^\circ$. Pentagons are distorted as well with various bond angles ranging from 104° to 112° . The minimum diameter of the "tubes" along the *c* axis, across the basal hexagons, is of 4.7 Å; the maximum diameter, corresponding to planes cutting Si₂₄ cages along their equator, is 10.6 Å. The ground-state valence electron charge density is mostly distributed along the bonds, very much as in normal silicon. Indeed these findings compare well with a previous LDA calculation of

the cubic clathrate sc-Si₄₆ [10], where the atomic volume and cohesive energies are found to be, respectively, 15% larger and about 0.09 eV smaller than in normal Si. An atomic volume increase of 17% and a difference in cohesive energy of 0.07 eV with respect to normal silicon have also been found in another calculation of fcc-Si₃₄ and sc-Si₄₆ [11]. Thus it appears that, within the numerical accuracy, hex-Si₄₀ is as stable as the other clathrates so far investigated.

The hex-Si₄₀ electronic structure (Fig. 2) has been calculated along the high-symmetry directions from the LDA Kohn-Sham eigenvalues using the self-consistent potential obtained with the set of three special *k* points. An indirect LDA energy gap of 1.03 eV is found, 0.44 eV wider than the indirect gap of normal Si obtained within the same computational scheme [17]. The minimum direct gap, located at 9/10 of the Γ -A edge, has an LDA value of 1.10 eV, only 70 meV larger than the absolute gap. The bottom of the conduction band, however, is located at the A point. In order to obtain the correct band gap, LDA results should be corrected with self-energy effects [18]. In a first approximation based on the "scissor operator" approach all the conduction bands are rigidly shifted to higher energies by Δ_g , as much as in normal Si ($\Delta_g = 0.6$ eV) [19], so that the real energy gap for hex-Si₄₀ is predicted to be about 1.6 eV. This value agrees with the calculated gaps of fcc-Si₃₄ and sc-Si₄₆ [10,11], where also a substantial widening was reported.

An empirical tight-binding (TB) calculation, which we performed using Sawada's parametrization [20], reproduces quite well the *ab initio* results, especially near the gap edges (Fig. 2, right), once the rigid shift of LDA conduction bands is applied. Actually the TB gap is almost direct due to the pronounced flatness of the gap-edge

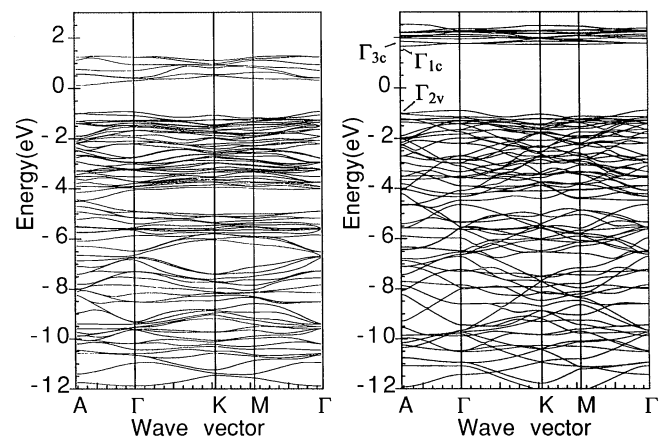


FIG. 2. Left panel: LDA band structure of hex-Si₄₀. The gap is indirect along Γ -A and it is 0.44 eV larger than in normal Si. The symmetry classification in Γ , in order of increasing energy for the near-gap bands, is Γ_{6v}^+ , Γ_{6v}^- , Γ_{5v}^- , Γ_{5v}^+ , Γ_{2v}^+ , Γ_{1v}^- for valence states and Γ_{2c}^- , Γ_{5c}^- , Γ_{1c}^+ , Γ_{3c}^- , Γ_{6c}^+ , Γ_{2c}^+ for conduction states. Right panel: TB results (see text). The wave vector in *K* is pointing along the *x* direction of Fig. 1.

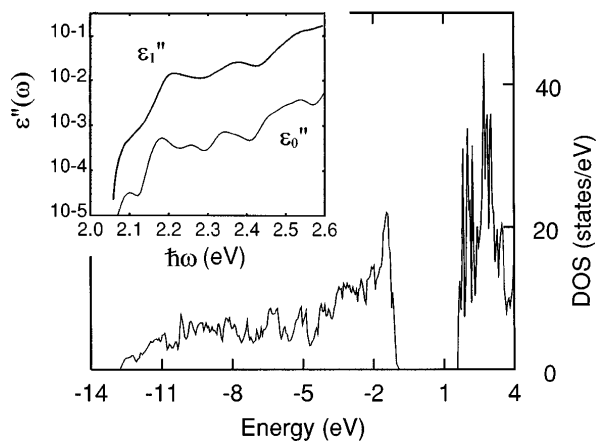


FIG. 3. Electronic DOS of hex-Si₄₀. The TB parametrization is used in order to achieve a full convergence in the k -space integration. In the inset, we show the zero (ϵ_0'') and one-phonon (ϵ_1'') contributions to $\epsilon''(\omega)$, as calculated from the LDA eigenstates corrected with the scissor operator.

bands. The TB parametrization, enabling us to work with a very large set of k points, has been used to calculate the density of states (DOS) of hex-Si₄₀ (Fig. 3).

Most of the states near the gap, which are involved in the PL transitions, are found to be spatially confined. A representation of the highest valence state at the A point (doubly degenerate Γ_{2v} band) is given in Fig. 4. In panel A we report the squared modulus of the LDA wave function in a plane perpendicular to the c axis and containing the Si-Si bonds surrounding the largest section of the tubes (equators of the Si₂₄ cages). In panel B, the same quantity has been averaged over the z direction, showing that there is almost no contribution from interstitial regions on any plane perpendicular to the c axis. An almost identical shape and localization is displayed by the two bands into which A_{2v} splits along the A - Γ direction (Γ_{1v}^- and Γ_{2v}^+ bands). Low energy unoccupied bands (Fig. 4, panels C and D) are also found to be spatially confined: the lowest conduction state at the A point, for example, is mostly localized inside the Si₂₄ and Si₂₆ cages, i.e., into “zero-dimensional” structures. Another unoccupied band, linking Γ_{5c}^- at Γ to Γ_{3c} at A , displays a large amplitude of the wave function on both internal and external surfaces of the tubular structures, suggesting a more one-dimensional confinement. This band is seen to give the largest contribution to the imaginary part of the dielectric function $\epsilon''(\omega)$ at frequencies below 2.8 eV (here, following Ref. [21], we take $\omega = \omega_{\text{LDA}} + \Delta_g/\hbar$). The transition from the bottom of the conduction band to the top of the valence band is dipole forbidden along the Γ - A edge. The same holds for transitions to the valence band immediately below (Γ_2^+ symmetry in Γ). Actually, we find no contribution to $\epsilon_0''(\omega)$ at the minimum direct gap. The first contributions to ϵ_0'' are instead predicted to appear at energies of 2.2–2.8 eV. They involve the three lowest conduction bands and the highest ten occupied bands.

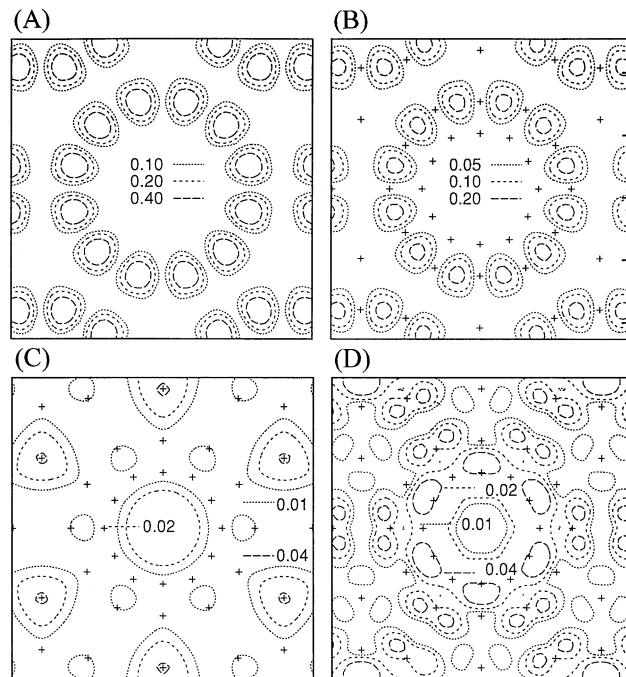


FIG. 4. Hex-Si₄₀ charge density contours at the A point for the highest valence state Γ_{2v} (a) a cut normal to the c axis in the equatorial plane of Si₂₄ cages; (b) averaged along the c axis and for the lowest conduction states; (c) the lowest state Γ_{1c} , whose density maxima occur at the center of Si₂₆ cages; (d) the immediately above doubly degenerate Γ_{3c} state, which gives a large contribution to ϵ'' . Crosses correspond to atomic positions projected onto the x - y plane.

We also evaluate the one-phonon contribution, $\epsilon_1''(\omega)$, following the procedure used by Hybertsen [3] for Si crystallites. In the present case, where the BZ is very small and the dispersion of optical phonons is weak, $\epsilon_1''(\omega)$ can be estimated under the simplifying assumption that only zone-center phonons, whose normalized DOS is $g(\omega^2)$, contribute, so that $\epsilon_1''(\omega)$ at $T = 0$ K is the convolution of $g(\omega^2)$ with $\epsilon_0''(\omega)$:

$$\epsilon_1''(\omega) = \frac{3d_0^2}{16\hbar\omega_0^2Mr_0^2} \int_0^{\omega_0} d\tilde{\omega} g(\tilde{\omega}^2) \epsilon_0''(\omega - \tilde{\omega}), \quad (1)$$

where d_0 is an average optical deformation potential (we take the experimental value for Si, $d_0 = 40$ eV [22]). M is the Si mass, $r_0 = 2.34$ Å an average bond length, and $\hbar\omega_0$ is the maximum phonon energy. For $g(\omega^2)$ we rescaled the spectrum of hex-C₄₀ as obtained from TB molecular dynamics [23]. The resulting $\epsilon_0''(\omega)$ and $\epsilon_1''(\omega)$ in the PL spectral region just above the gap are plotted in the inset of Fig. 3. There is a striking similarity with Hybertsen’s calculation for ~ 20 Å crystallites in both shape and order of magnitude of the two dielectric functions, so that Hybertsen’s conclusions regarding the photoluminescence yield of small silicon crystallites apply equally well to the present crystalline silicon form.

In conclusion, we have computed the structural and electronic properties of a new form of silicon with a

unit cell of 40 atoms, and perfect fourfold coordination. This material, which is predicted to be as stable as the cubic silicon clathrates (Si_{46} , Si_{34}), is a semiconductor with a gap more than 0.4 eV larger than normal silicon. Both LDA and TB calculations yield gap-edge bands with a dispersion of less than 0.5 eV, also due to the small size of the BZ. The analysis of the dipole matrix elements between valence and conduction states and the study of their spatial localization reveals that low-lying excitations, responsible for the onset of optical absorption and possibly concerned by photoluminescence, involve mainly electronic states which are spatially confined. The existence of low-dimensional electronic states, together with the substantial widening of the gap, make the dielectric properties of hex- Si_{40} on the PL spectral region surprisingly similar to those of silicon crystallites and, ultimately, of porous silicon. If synthesized, hex- Si_{40} would then share the great technological interest of π -Si for optoelectronic applications.

We are grateful to Professor M. Scheffler for useful discussions, and to Dr. M. Bernasconi for a critical reading of the manuscript.

[1] L. T. Canham, *Appl. Phys. Lett.* **57**, 1046 (1990).
 [2] D. J. Lockwood, *Solid State Commun.* **92**, 101 (1994).
 [3] M. Hybertsen, *Phys. Rev. Lett.* **72**, 1514 (1994).
 [4] C. Delerue, M. Lannoo, G. Allan, and E. Martin, *Thin Solid Films* **255**, 27 (1995).
 [5] G. Onida and W. Andreoni, *Chem. Phys. Lett.* **243**, 183 (1995).
 [6] J. L. Gavartin, C. C. Matthai, and I. Morrison, *Thin Solid Films* **255**, 39 (1995).
 [7] F. Buda, J. Kohanoff, and M. Parrinello, *Phys. Rev. Lett.* **69**, 1272 (1992); see also L. Dorigoni, O. Bisi, F. Bernardini, and S. Ossicini, *Phys. Rev. B* **53**, 4557 (1996).

[8] R. Car and M. Parrinello, *Phys. Rev. Lett.* **55**, 2471 (1985).
 [9] R. Stumpf and M. Scheffler, *Comput. Phys. Commun.* **79**, 447 (1994).
 [10] S. Saito and A. Oshiyama, *Phys. Rev. B* **51**, 2628 (1995).
 [11] G. B. Adams, M. O'Keefe, A. A. Demkov, O. Sankey, and Y. Huang, *Phys. Rev. B* **49**, 8048 (1994).
 [12] H. Kawaji, H. Horie, S. Yamanaka, and M. Ishikawa, *Phys. Rev. Lett.* **74**, 1427 (1995).
 [13] G. Benedek, E. Galvani, S. Sanguinetti, and S. Serra, *Chem. Phys. Lett.* **244**, 339 (1995).
 [14] We used the public domain CP code *fhi94md*, available via ftp at the Internet node xtheo21.RZ-Berlin.MPG.DE:/pub/physics. A previous version of this code is described in Ref. [9].
 [15] G. Bachelet, D. R. Hamann, and M. Schlüter, *Phys. Rev. B* **26**, 4199 (1982).
 [16] D. J. Chadi and M. L. Cohen, *Phys. Rev. B* **8**, 5747 (1973).
 [17] For the sake of comparison, it is noticeable that in the case of similar clathrates, but based on carbon instead of silicon, DFT-LDA calculations show the opposite effect: the gap closes with respect to diamond [R. Nesper, K. Vogel, and P. E. Blochl, *Angew. Chem., Int. Ed. Engl.* **32**, 701 (1993)].
 [18] See, for example, M. S. Hybertsen and S. G. Louie, *Phys. Rev. Lett.* **55**, 1418 (1985); *Phys. Rev. B* **34**, 5390 (1986); R. W. Godby, M. Schlüter, and L. J. Sham, *Phys. Rev. Lett.* **56**, 2415 (1986); *Phys. Rev. B* **37**, 10 159 (1988).
 [19] An evaluation of the consequences of the states localization, which is discussed below, on these self-energy corrections, calls for an accurate calculation of the quasi-particle band structure of hex- Si_{40} , which is, however, beyond the scope of the present work.
 [20] S. Sawada, *Vacuum* **41**, 612 (1991).
 [21] R. Del Sole and R. Girlanda, *Phys. Rev. B* **48**, 11 789 (1993).
 [22] A. Blacha, H. Presting, and M. Cardona, *Phys. Status Solidi (b)* **126**, 11 (1984).
 [23] G. Benedek and L. Colombo, in "Cluster Assembled Materials," edited by K. Sattler (TransTech Publ., Winterthur, 1996), p. 1–27.